

Thermal degradation of acrylonitrile–butadiene–styrene (ABS) blends

B.E Tiganis^{a,*}, L.S Burn^a, P Davis^a, A.J Hill^b

^aCSIRO Building, Construction and Engineering, PO Box 56, Highett, Victoria 3190, Australia

^bCSIRO Manufacturing Science and Technology, Victoria, Australia

Received 24 October 2001; received in revised form 18 January 2002; accepted 27 January 2002

Abstract

This work investigates the accelerated thermal degradation of acrylonitrile–butadiene–styrene (ABS) due to aging at elevated temperatures (> 80 °C). The impact resistance is shown to decrease dramatically beyond a critical aging time at 120 °C and this reduction strongly depends on surface property modifications during aging. Visual examination of specimen cross-sections after aging, verifies that (dis)colouration is limited to a surface layer, which is characteristic of degradation where oxygen diffusion into the bulk is limited. Degradation is supported by chemiluminescence assessment, which shows a rapid depletion of residual stabiliser within this layer as compared to the bulk polymer. Micro-indentation measurements also indicate that degradation causes an increase in Young's modulus at the specimen surface, which in turn promotes brittle failure. It is proposed that a critical depth of degradation (approximately 0.08 mm) forms on the surface of ABS due to aging. Applied loading initiates microcracks in this degraded layer, which propagate rapidly, causing bulk failure. Absorbance bands from Fourier transform infra-red spectroscopy indicate that surface degradation proceeds by chain scission and cross-linking in the polybutadiene (PB) phase of aged ABS specimens. Cross-linking is also supported by positron annihilation lifetime spectroscopy, which shows a decrease in free volume sites at the surface of aged specimens. Dynamic mechanical thermal analysis also supports the occurrence of cross-linking, as shown by an increase in the glass transition temperature of the PB phase after aging. Although degradation in the styrene–acrylonitrile (SAN) phase is less significant to the reduction in overall mechanical properties of ABS compared to the PB phase, an assessment of SAN copolymer indicates that heat aging decreases impact resistance. The contribution of SAN to the overall mechanical properties of ABS is also reflected by aging ABS specimens at temperatures just below the glass transition of the SAN phase (~ 112 °C). The mechanism of thermal degradation is shown to be non-Arrhenius and governed by diffusion-limited oxidation. The long-term impact strength of ABS at ambient temperature is extrapolated from short-term data at elevated temperatures. As temperature and aging time influence degradation, it is proposed that at ambient service temperatures (40 °C), the degradation mechanism differs to that at elevated temperatures, and comprises both surface and bulk polymer degradation effects. © 2002 Elsevier Science Ltd. All rights reserved.

Keywords: ABS; Degradation; Durability; Heat aging; Physical properties; Mechanical properties

1. Background

The durability of acrylonitrile–butadiene–styrene (ABS) polymers is important in many applications and depends on composition, processing and operating conditions, environmental weathering, heat aging and installation damage. The availability of a durability prediction model for ABS would allow material types to be selected according to their expected environmental

and operating conditions, and would significantly reduce the risk of in-service failures.

Specific microstructural aspects of a polymer often facilitate thermal oxidation. In the case of ABS, hydrogen abstraction by oxygen is thermodynamically favourable due to the presence of tertiary substituted carbon atoms in the PB phase. The presence of sufficient thermal energy activates hydrogen abstraction to initiate oxidation, and accelerates the overall process of degradation. After periods of exposure to heat and oxygen, the mechanical properties of ABS such as impact strength and elongation to break, deteriorate as a consequence of this polymer degradation, inducing premature failure

* Corresponding author. Tel.: +61-3-9252-6000; fax: +61-3-9252-6244.

E-mail address: bill.tiganis@dbce.csiro.au (B.E Tiganis).

[1]. The literature cites various explanations for the degradation of ABS due to heat aging. Several researchers state that thermo-oxidative degradation of ABS is confined to the rubbery PB phase, while others propose that property degradation is due to a combination of physical aging in the SAN phase and oxidation of the PB phase [2–5]. Shimada and Kabuki [3] proposed that thermo-oxidative degradation occurred in the rubber phase of unstabilised ABS film, leading to the formation of hydroperoxides. Degradation was thought to occur by hydrogen abstraction from the α carbon next to the *trans*-1,4 and 1,2 unsaturations in the PB phase, producing hydroperoxide radicals. The rate of this reaction was said to follow Arrhenius-type kinetics, with rate constants and reaction orders determined from the formation rate of carbonyl and hydroxyl products, as monitored by Fourier transform infra-red (FTIR) spectroscopy. In contrast, Wyzgoski [4] states that annealing ABS below the glass transition temperature (T_g) of its SAN phase (physical ageing), produces molecular conformations which embrittle the polymer, significantly decreasing tensile elongation properties. Below its glass transition temperature, the SAN microstructure adopts an energetically unfavourable state driving towards equilibrium via molecular motion [6]. The transformation between a glass and an amorphous polymer involves a kinetic process of polymer molecule mobility. By providing thermal energy during the physical aging (annealing) process, a glass tends to equilibrate its polymer microstructure [4,7]. When heating annealed polymers, as the temperature increases towards T_g , the rate of the kinetic process is retarded in comparison to unannealed polymers [6], and thus, in comparison, the rate of change in $\tan \delta$ decreases as T_g is approached. On a macro level, this physical aging process increases stiffness and yield a stress — in fact, yield stress is increased above craze stress such that brittle fracture is favoured over yielding.

In this study, thick specimens of stabilised ABS were aged at elevated temperatures in order to study the effects of heat aging on mechanical properties. The study does not consider environmental effects such as the migration and leaching of stabiliser that may occur in typical outdoor infrastructure applications.

2. Experimental program

The ABS polymer morphology under investigation was comprised of a SAN-graft-PB bimodal matrix with dispersed ungrafted PB polymer.

2.1. Heat aging

Commercial ABS pipe resin and pure SAN copolymer, in the form of impact (conforming to AS 1146.1

[8]) and tensile (conforming to AS 1145 [9]) specimens were aged in a Qualtex Solidstat Universal 2000 series oven. Specimens were exposed to a range of temperatures over different time periods. Oven conditions were maintained as required by ISO 188 [10]. Initial heat aging experiments on ABS were conducted at 90 °C (with the specimen notched after heat aging) and 120 °C (using both unnotched and notched specimens). In each case, aging continued for 672 h. Additional heat aging trials were conducted at 80, 90, 105, 110 and 120 °C for unnotched ABS specimens (up to 672 h), and at 80, 90 and 105 °C for SAN (up to 1008 h). Samples were removed periodically during these times for mechanical and physical assessment.

2.2. Mechanical property assessment

Instrumented impact analyses were performed on ABS and SAN specimens using a Radmana impact tester, in accordance with AS 1146.1 [8]. Young's modulus and ultimate elongation were assessed for both as-produced and aged ABS and SAN specimens on an Instron 5565 screw-driven tensile tester (5 KN) using pneumatic grips (500 kPa grip pressure) according to AS 1145 [9]. ABS specimens aged for 168 h at 120 °C and as-produced ABS specimens were mechanically milled to a depth of 0.7 mm on all surfaces to remove the degraded layer and allow surface effects to be assessed. To measure T_g and loss modulus of ABS, specimens were sectioned prior to heat aging, to the required dimensions for thermo-mechanical property assessment. T_g and loss moduli were measured using a Rheometrics Scientific Solids Analyser RSA II DMTA, for both the rubber polybutadiene phase and the rigid SAN phase of ABS after heat aging at 120 and 90 °C. To determine the effects of aging on surface properties, microhardness assessments were conducted on ABS specimens as-produced and also aged at 90 and 120 °C. A UMIS 2000 ultra micro-indentation system (using a spherical indenter of 20 μm radius) was used to apply a load/partial unload cycle (with a 0.1 s time period) up to a maximum load of 50 mN.

2.3. Microstructural property assessment

To investigate aging effects on polymer microstructure, FTIR spectroscopy was used to identify the characteristic infra-red absorptions of vinyl groups in as-produced ABS and carbonyl and hydroxyl absorptions due to the oxidation species of ABS. Using a 20 μm thick microtomed cross-section of aged ABS (672 hours), local regions (100 \times 100 μm) were analysed at the edge of the section (corresponding to the specimen surface) and within the centre of the microtome (corresponding to the bulk polymer). Optical transmission mode was used with microscope stage control and

imaging to allow visual identification of the section. Positron annihilation lifetime spectroscopy (PALS) analysis was conducted on ABS aged at 90 and 120 °C, and SAN aged at 90 °C to investigate the effects of heat aging on the molecular level packing features of the polymer (e.g. free volume). Analyses were conducted in the bulk of aged ABS by removing the surface layer (0.7 mm) by mechanical milling prior to assessment. An Atlas CL 400 chemiluminescence instrument was used to investigate the depletion of residual stabiliser in ABS after aging. Both surface and bulk samples (20 µm) from an ABS specimen aged at 120 °C were analysed at an isothermal temperature of 180 °C in oxygen, after a nitrogen pre-phase. The onset of polymer degradation, or the oxidation induction time (OIT), due to stabiliser depletion was recorded for each sample.

3. Thermal degradation at the surface of heat aged ABS specimens

Fig. 1 shows the variation in impact strength with aging time for ABS specimens that were notched *after* aging at 90 and 120 °C. As shown, impact strength is effectively independent of aging time at 90 °C, with only a slight loss was observed at 120 °C. In contrast, however, the impact strength of unnotched ABS specimens aged at 120 °C decreases rapidly after an aging time of 168 h, as shown in Fig. 2 where the initial impact value of 245 kJ/m² decreases to a plateau of approximately 30 kJ/m². Since notching after heat aging removes the surface structure of a specimen, the results in Figs. 1 and 2 indicate that failure under impact is critically dependent on the condition of the surface layer in ABS. The influence of surface degradation on bulk mechanical properties is evident by comparing the tensile properties of ABS specimens with their surfaces intact and removed. The tensile elongation energy to break for aged ABS specimens after the aged surface is

removed (0.7 mm) is restored to that of an as-produced specimen.

As shown in Fig. 3, ABS specimens aged at 120 °C develop a brown colouration at the polymer surface. A cross-sectional examination of these specimens reveals that the colouration of the polymer is limited to the surface even after heat aging for several months. This reinforces previous research by Wolkowicz and Gagar [1], which proposes that the loss of impact strength for aged ABS specimens is controlled by a critical depth of degraded surface polymer. Referring back to Fig. 2, the transition in impact resistance corresponds to a surface layer depth of approximately 0.08 mm. Further exposure does not reduce impact strength, even though the depth of the coloured layer continues to increase to 0.3 mm after 672 h. This critical layer depth of 0.08 mm is also in agreement with the lower end of previously reported values between 0.07 and 0.2 mm [1].

3.1. Mechanical properties at the surface of aged ABS specimens

The effects of aging on the surface mechanical properties of ABS were investigated using a microhardness tester. Microhardness assessment measures the force required to impress an indenter to a fixed depth through the specimen surface. The measured force is proportional to the surface elastic modulus of ABS after correcting for local plastic deformation. Whilst Fig. 4 shows that the elastic modulus of ABS aged at 90 °C does not differ significantly from that of as-produced ABS (1500 MPa), the modulus of ABS aged at 120 °C increases by 300% to 4500 MPa. The initial decreases in elastic moduli shown in Fig. 4 are due to specimen surface imperfections. It is proposed that this increase in local modulus after aging is associated with cross-linking and reductions in free volume in the surface layer (discussed later), and is consistent with the decrease in impact resistance shown in Fig. 2.

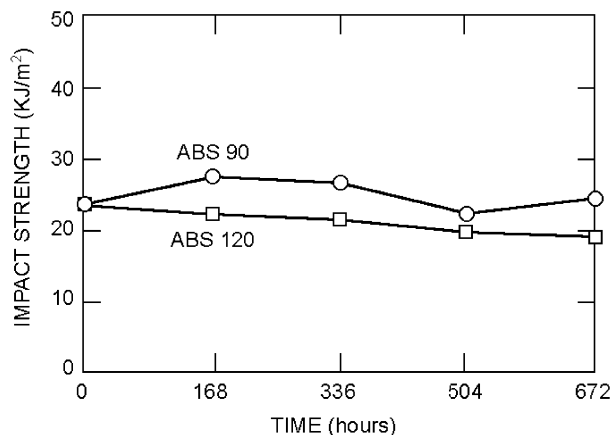


Fig. 1. Impact strength of notched ABS as a function of ageing time at 90 and 120 °C.

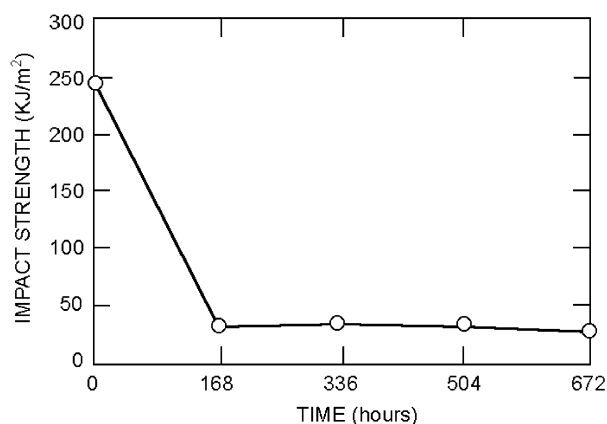


Fig. 2. Impact strength of unnotched ABS as a function of ageing time at 120 °C.

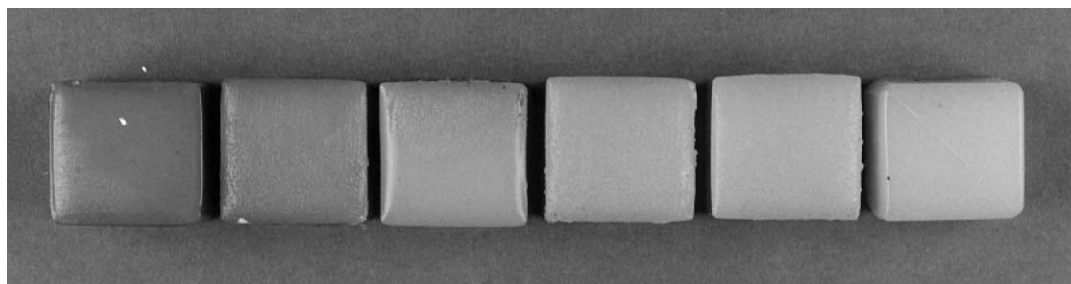


Fig. 3. Colouration of ABS as a function of ageing time (left, 168 h; far right, 0 h) at 120 °C.

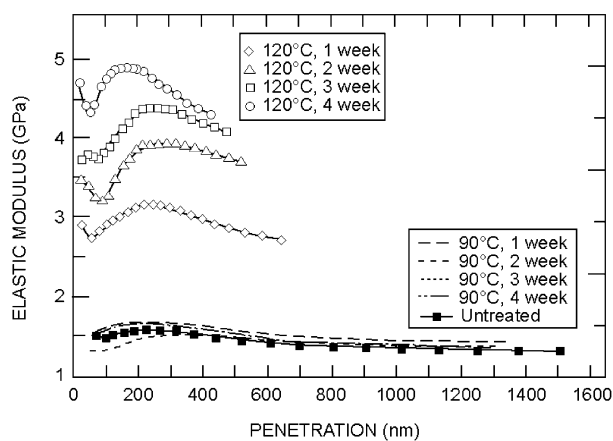
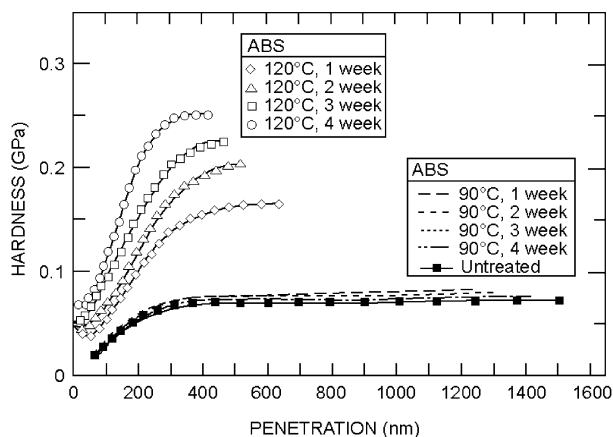


Fig. 4. Hardness (top) and elastic modulus (bottom) measures of as-produced and ABS aged at 90 and 120 °C.

3.2. Chemical properties at the surface of aged ABS specimens

Many researchers attribute the colouration of ABS to thermal aging, during which radical scavengers are thought to couple with peroxy radicals formed during degradation reactions [11]. Degradation and subsequent discolouration in ABS is confined to the surface of the specimen and is controlled by the rate of oxygen diffusion through the polymer. As a degraded layer forms, polymer density increases limiting the diffusion of oxygen.

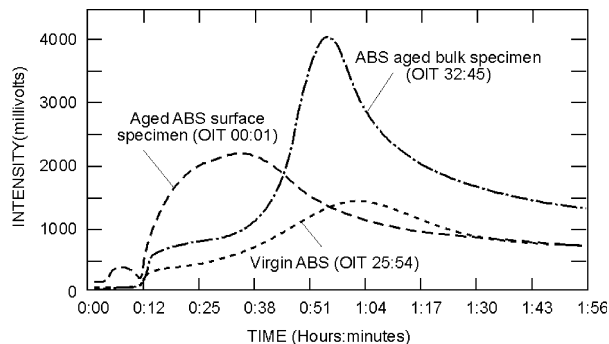


Fig. 5. Chemiluminescence oxidation induction time (OIT) data for the surface and bulk polymer of ABS aged for 168 h at 120 °C.

Therefore, the rate of degradation through a thick ABS section decreases over time. It follows that the residual stabiliser that is incorporated in commercial grades of ABS must be depleted at the specimen surface as oxidation occurs [11–13]. This is verified by the plots in Fig. 5 showing chemiluminescence peaks for ABS polymer aged at 120 °C for 168 h. The voltage recorded in chemiluminescence assessment is directly related to the light intensity created by decaying hydroperoxides in degradation reactions [13]. As shown, the oxidation induction time (indicating the quantity of residual stabiliser in the polymer) is significantly lower at the specimen surface. In contrast, the signal for the bulk polymer specimen appears similar to that obtained from an as-produced specimen. FTIR spectroscopic analysis can also be used to compare aging-induced chemical changes in microtomed sections of ABS. Fig. 6 shows FTIR spectra from the surface (upper spectrum) and bulk (lower spectrum) of an ABS specimen after aging at 120 °C for 168 h. As shown, the spectrum from the bulk polymer is similar to a trace that is commonly observed for as-produced ABS. There is no observed change in the characteristic infra-red absorptions of ABS and no evidence of chemical degradation products. In contrast, however, spectral changes are clearly observed at the surface of the aged polymer, in particular the carbonyl peak at 1724 cm^{-1} , indicating changes in chemical structure associated with oxidation.

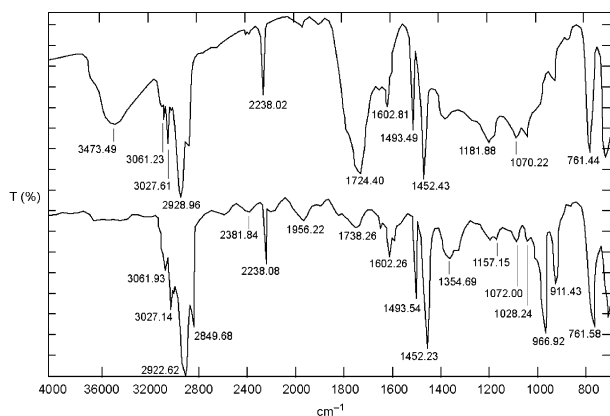


Fig. 6. Transmission FTIR spectra of ABS aged at 120 °C. Upper spectrum represents analysis at the surface and the lower spectrum in the bulk ABS polymer.

4. Phase degradation of ABS specimens aged at elevated temperatures

ABS consists of a bimodal polymer system in which non-grafted polybutadiene particles are dispersed in a SAN-graft-polybutadiene matrix phase. Whilst the loss of mechanical properties in ABS is often attributed to thermo-oxidative degradation in the PB phase only, thermo-oxidative degradation and physical aging can also occur in the SAN phase [2–5].

4.1. Degradation in the PB phase

Thermal degradation of the PB phase in ABS is initiated by hydrogen abstraction from carbon atoms in an α position to unsaturated bonds. The abstraction generates radicals which, in the presence of oxygen, lead to the formation of carbonyl and hydroxyl products. Following a reaction scheme proposed by Shimada and Kabuki [3], degradation products may decompose further to create various polymer radicals, which facilitate cross-linking and/or form degradation products such as polymer peroxides. These polymer degradation products form microstructural inconsistencies, which may act as stress concentration sites. Thermo-oxidative degradation of the PB phase can also increase polymer density by cross-linking. The corresponding increase in Young's modulus precipitates brittle behaviour, reducing the contribution of PB to the overall toughening mechanisms of localised shear yielding and crazing in ABS [14]. This degradation mechanism is verified by the FTIR spectra for aged ABS in Fig. 6. The absorbance bands at 966.92 and 911.43 cm^{-1} correspond to the trans C=C unsaturation (vinyl) in polybutadiene, and the 1,2 butadiene terminal vinyl C–H band respectively. The surface spectrum for aged ABS shows a significant decrease in these bands, indicating chemical changes in the PB microstructure, which are probably attributed to chain scission and cross-linking. Furthermore, degrada-

tion of the PB phase at the surface forms hydroperoxide species, as indicated by the carbonyl (1724.4 cm^{-1}) and hydroxyl (3473.49 cm^{-1}) absorbances in the spectrum [2–5]. Degradation of the PB phase by cross-linking would also be expected to reduce polymer chain mobility and decrease free volume. This reduction in free volume can be detected using PALS, which monitors the lifetimes of positrons in the polymer [15]. Fig. 7 shows PALS results from the surface of an ABS specimen aged at 120 and 90 °C together with SAN copolymer aged at 90 °C. Whilst the relative free volume fraction, indicated by oPs intensity (I_3), for ABS and SAN aged at 90 °C is approximately constant, ABS aged at 120 °C shows a significant reduction in I_3 with increasing aging time. As shown in Fig. 8, the relative size of free volume sites, represented by oPs lifetime (τ_3) also decreases with increasing aging time for ABS specimens aged at 120 °C. In contrast, (τ_3) for ABS or SAN aged at 90 °C does not change significantly. The decreasing values of I_3 and τ_3 are interpreted as a reduction in free volume due to cross-linking reactions in the PB phase. The presence of free radicals or other electron or positron scavengers due to the degradation process can also cause a decrease in the value of I_3 [16]. Further work is progressing to determine the relative contributions of cross-linking and the presence of scavengers to the observed changes in these PALS parameters.

Molecular chain cross-linking will increase the T_g of the PB phase, which can be measured by dynamic mechanical thermal analysis (DMTA). DMTA monitors the phase lag (expressed by the 'tan δ ' parameter) between an imposed cyclic stress and a recorded cyclic strain as specimen temperature increases. At a temperature $T = T_g$, a peak in tan δ is attained which corresponds to a transition in molecular conformation from a glassy (rigid) to a rubbery state. It follows that cross-linking in the PB phase will increase T_g , by increasing the thermal energy required to free polymer molecules from additional constraint. As shown in Table 1, whilst T_g remains unchanged after aging at 90 °C, aging at 120 °C produces an increase in T_g with increasing aging time. The phase lag between imposed stress and strain (tan δ) can also be written as the ratio between two moduli E''/E' . E'' is often referred to as the 'loss modulus', and E' as the 'storage modulus' since they relate to the amount of energy that is dissipated and stored during each loading cycle. Referring back to Table 1, the increase in T_g due to cross-linking can also be interpreted by the temperature at which a peak in E'' is attained. For specimens aged at 120 °C, maximum energy dissipation generally occurs at a temperature that increases with aging time. The influence of cross-linking in the PB phase is also evident in the Young's modulus of aged ABS specimens. As shown in Fig. 9, whilst aging at 120 °C produces an increase of 40% in

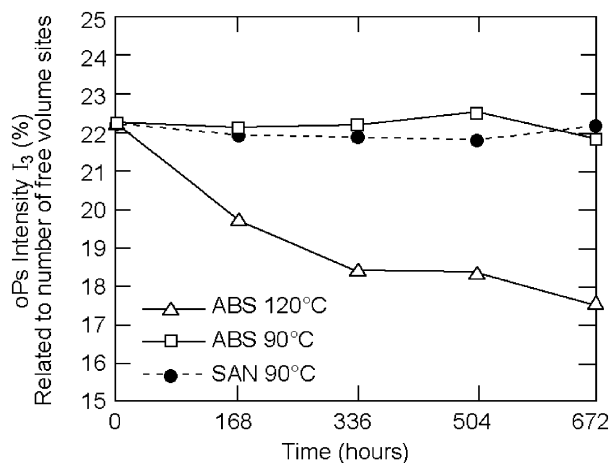


Fig. 7. The oPs intensity for ABS aged at 90 and 120 °C and SAN aged at 90 °C. The population standard deviation on I_3 is $\pm 0.3\%$ absolute.

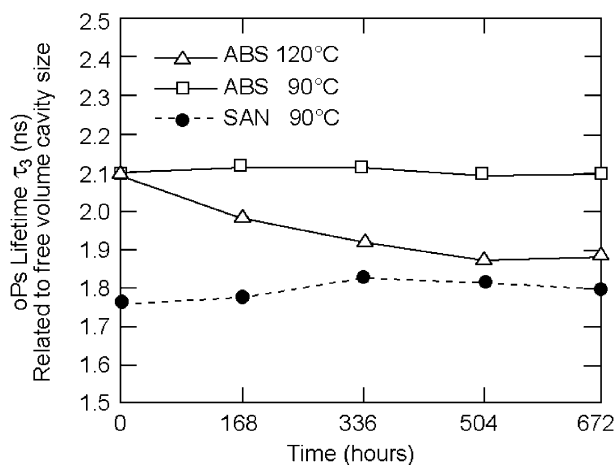


Fig. 8. The oPs lifetime for ABS aged at 90 and 120 °C and SAN aged at 90 °C. The population standard deviation on τ_3 is $\pm 0.03\%$ ns.

Young's modulus, aging at 90 °C results in only a slight increase. Similar to the impact tests in Fig. 2, this aging-induced increase in Young's modulus also influences failure mode at relatively low loading rates. Fig. 10 shows a typical stress–strain curve for as-produced and aged ABS at 90 and 120 °C, from a tensile test at 10

mm/min. Although the ultimate elongation decreases for ABS aged at 90 °C, post-yield drawing is still observed, as indicated by the decrease in load before failure. In comparison, aging of ABS at 120 °C eliminates this load drop and failure occurs in the elastic regime. Clearly, aging (and subsequent cross-linking in the PB phase) increases Young's modulus and results in a ductile–brittle transition in failure mode. This change in failure mechanism may be associated with a decrease in fracture toughness (K_{IC}) of the polymer with aging, as has been observed with PVC [17], however, this avenue is still to be fully explored.

In summary, ABS heat stabiliser is depleted with increasing aging time and aging temperature, and chemical degradation in the PB microstructure precipitates mechanical failure. As shown in Fig. 11, the loss of impact strength of unnotched specimens occurs at a transitional aging time that decreases with increasing aging temperature. Similarly, Fig. 12 shows that the tensile energy to break properties of ABS aged between 90 and 120 °C, significantly deteriorate as the temperature and time of aging increases, as do the tensile strain properties. The decrease in tensile properties is similar to that reported by Tavakoli [18], who found a 30–70% reduction in tensile strength for ABS aged at 120 °C.

4.2. Degradation in the SAN phase

The type and extent of thermal degradation in the SAN phase of ABS depends on the proximity of the aging temperature to the glass transition temperature of SAN ($T_g \sim 113$ °C). Aging at temperatures below T_g causes physical aging [4,19], and at temperatures greater than T_g , thermo-oxidative degradation is observed. Although both physical aging and thermo-oxidative degradation of the SAN phase may occur, their contribution to the overall deterioration of ABS mechanical properties is comparatively insignificant compared to the effects of thermo-oxidative degradation in the PB phase [13,19]. For example, pure SAN copolymer has an impact resistance of ~ 27 kJ/m² compared to 250 kJ/m² for ABS. However, similarly to ABS as shown in Fig. 13, the impact resistance of SAN copolymer

Table 1
Temperature at peak E'' and peak $\tan \delta$ values of the polybutadiene phase in ABS as a function of aging time at 90 and 120 °C

Ageing period (hours)	90 °C		120 °C	
	Peak $\tan \delta$ temp. (°C)	Peak loss modulus (E'') temp. (°C)	Peak $\tan \delta$ temp. (°C)	Peak loss modulus (E'') temp. (°C)
0	–86	–85	–86	–85
168	–86	–85	–79	–77
336	–85	–86	–76	–72
504	–85	–86	–81	–81
672	–85	–86	–81	–81

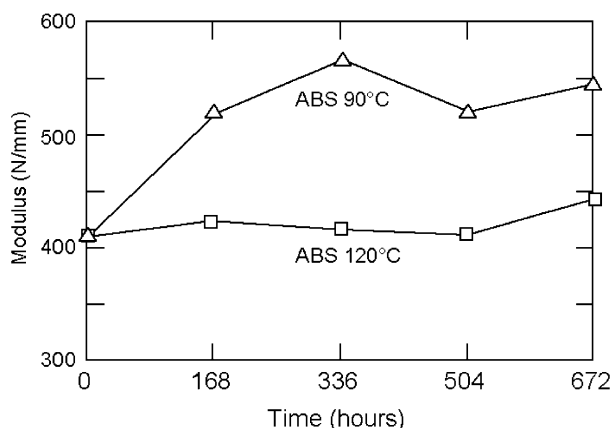


Fig. 9. Young's modulus of ABS aged at 90 and 120 °C.

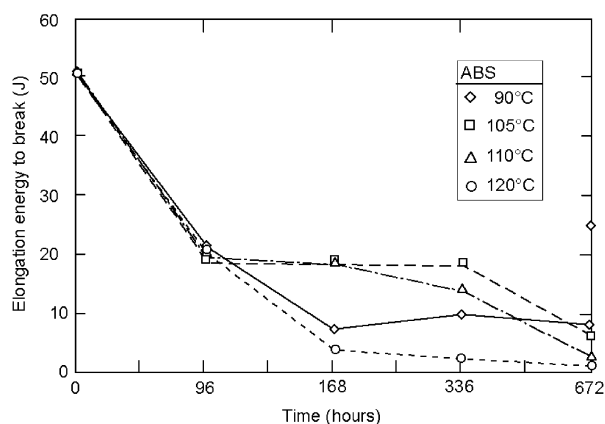


Fig. 12. Ultimate tensile elongation energy for ABS as a function of ageing time at 90, 105, 110 and 120 °C.

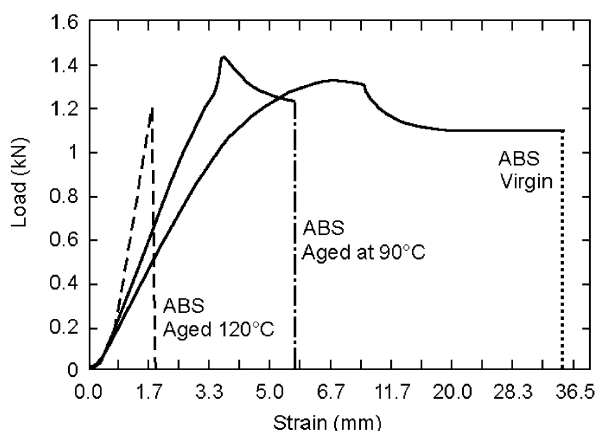


Fig. 10. Stress-strain curve for as-produced ABS and ABS after ageing at 90 and 120 °C.

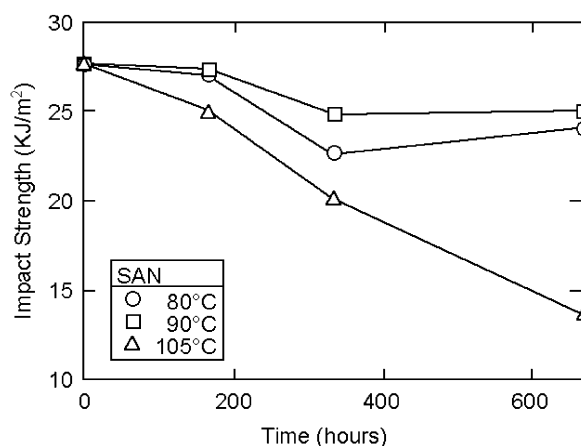


Fig. 13. Impact strength of unnotched SAN as a function of ageing time at 80, 90 and 105 °C.

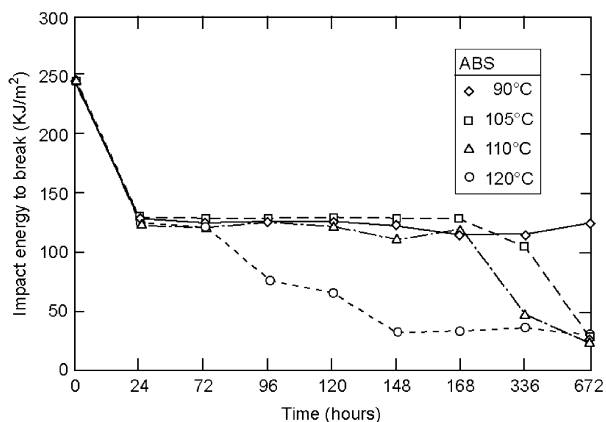


Fig. 11. Impact strength of unnotched ABS as a function of ageing time at 90, 105, 110 and 120 °C.

decreases after aging, with a reduction from 27 kJ/m² to 14 kJ/m² occurring after aging at 105 °C for 672 hours. Although this temperature is below T_g for SAN and physical aging may occur, thermo-oxidative degradation is also evident by specimen discolouration [11]. According to Wyzgoski [4], aging of the SAN phase and

its effects on the mechanical properties of ABS is assumed to be reversible by heating above the glass transition of the SAN phase. It is proposed that at the temperatures analysed in this study, chemical degradation such as cross-linking in the SAN phase does not occur and that physical aging is the controlling mechanism, as discussed below.

When glassy polymers such as SAN are aged at temperatures below the glass transition, they are said to be annealed or physically aged. Physical aging rearranges molecules from an unordered state, formed initially by quench cooling, to an equilibrated or uniform glassy state [20]. Whilst Fig. 7 illustrates that this reordering reduces free volume similar to cross-linking in the PB phase [20], physical aging of the SAN phase is independent of oxygen diffusion and is not limited to the surface of thick ABS specimens. The glass transition in an amorphous polymer occurs by a kinetic process of molecular mobilisation as temperature increases. In general, as T_g is approached from below, the rate of this kinetic process is auto-retarded [4]. Therefore, physically aging a glass by applying thermal energy tends to

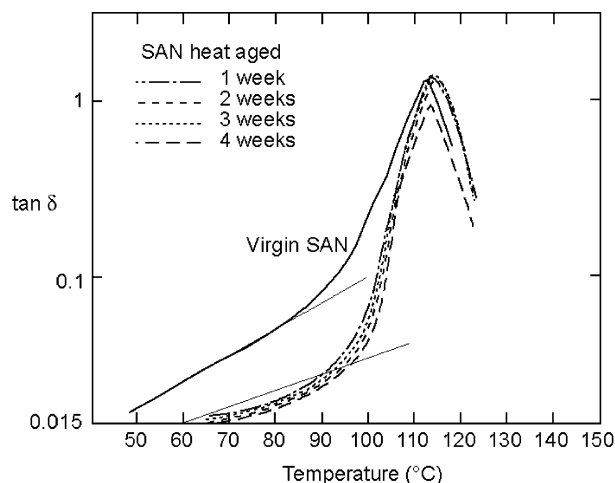


Fig. 14. $\tan \delta$ parameters of the SAN phase of ABS aged at 90 °C. Tangents indicate a decrease in the rate of transition for aged SAN copolymer.

equilibrate the polymer microstructure and decrease the initial rate of the glass transition in comparison to an unaged glass [4,5,7]. The influence of physical aging in SAN is illustrated in Fig. 14. As expected, the initial slope of the $\tan \delta$ curve for aged ABS is lower than that for as-produced specimens in the approach to the glass transition of the SAN phase. Table 2 compares the E'' and $\tan \delta$ parameters for the SAN phase in as-produced ABS and ABS aged at 90 °C. As shown, whilst there is only a slight increase in T_g , the temperature at which the maximum loss modulus E'' is attained increases significantly with aging time. Similar to the influence of cross-linking in the PB phase, physically aging SAN creates sufficient molecular order to require an increase in thermal energy to overcome constraint. Referring back to Fig. 9, physical aging of the SAN phase can also account for the slight increase in Young's modulus in ABS specimens aged at 90 °C. Previous research also suggests that the aging-induced changes in ultimate elongation (Fig. 12) and yield stress (Fig. 10) in ABS can be partly attributed to SAN physical aging [21–23].

5. Predicting long-term mechanical stability of ABS at ambient conditions from heat aging results at elevated temperatures

Although the degradation of ABS and the loss of mechanical properties is strongly temperature dependent, the kinetics of degradation are unlikely to follow an Arrhenius law over a large temperature range. Whilst the Arrhenius equation is often used to model degradation kinetics, the extent of diffusion-limited oxidation (DLO) may change with time and temperature in relatively thick specimens. Time and temperature of aging influence the rate of formation and thickness of the degraded surface layer, and therefore the extent to

Table 2
Temperature at peak E'' and $\tan \delta$ values for the SAN phase of ABS aged at 90 °C

Ageing period (h)	Peak $\tan \delta$ temp. (°C)	Peak loss modulus (E'') temp. (°C)
0	113	103
168	114	108
336	114	106
504	114	106
672	113	107

which degradation may occur in the bulk polymer. At ambient service temperatures, the mechanism of degradation may differ to that at elevated temperatures, comprising both surface and bulk polymer degradation effects. Whilst Clough et al. [13] found that the Arrhenius equation predicts tensile elongation properties for aging of SBR polymers, the tensile strength of the total specimen cross-section geometry does not take into account the DLO effects occurring. Furthermore, whilst the Arrhenius relationship may model the loss of one mechanical property with aging, it may not capture other properties.

Fig. 15 shows normalised impact strength [impact energy (I)/initial impact energy (I_o)] against aging time for aged ABS specimens. By plotting three levels of deterioration ($I/I_o = 0.25, 0.5, 0.75$) against the reciprocal of temperature (Fig. 16), it is apparent that for the initial stages of degradation ($I/I_o = 0.75$) and at lower temperatures, the curve is not linear. As shown by the slope of the curve, the degradation process requires a different activation energy at this stage compared to later stages. For the Arrhenius relationship to be applicable, the activation energy for the degradation reaction at different stages or levels of degradation must not change. Tensile energy to break results were also found to deviate from Arrhenius behaviour. It appears that two different degradation profiles may exist for thermo-oxidative degradation of ABS. For temperatures below 90 °C, such as the ambient operating temperature (in this case, assumed to be 40 °C), degradation may occur consistently throughout ABS and follow an Arrhenius description. However, it is proposed that DLO effects control degradation at elevated temperatures, with oxidation occurring at the specimen surface.

In the absence of a physical degradation law, a simple extrapolation of short-term impact properties at elevated temperatures allows the prediction of long-term impact strength at ambient conditions (Fig. 17). However, as suggested previously, discrepancies may be expected in practice due to the influence of aging time and temperature over the formation rate of a degraded layer. Future work will focus on modelling the kinetics of degraded layer formation, and the use of a fracture

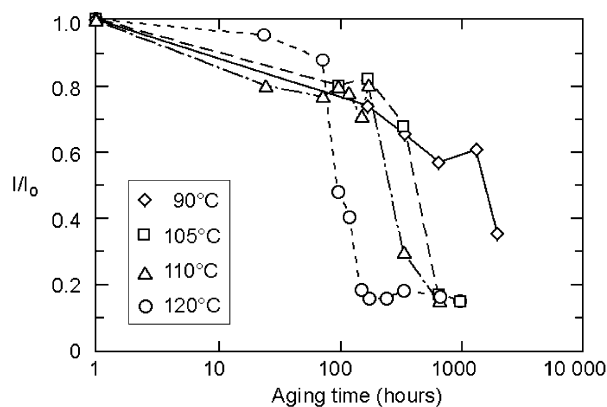


Fig. 15. Normalised impact strength values (impact energy at specific time/initial impact energy) plotted against time.

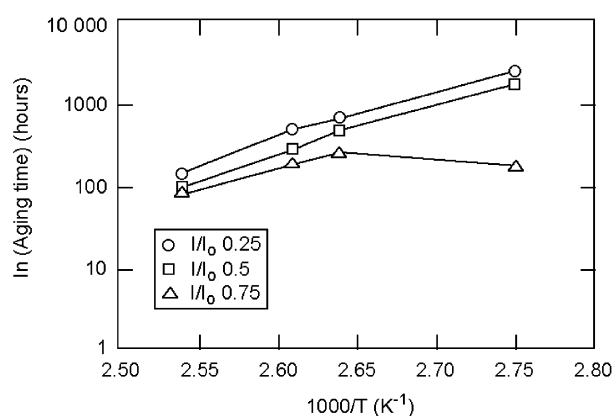


Fig. 16. Time of aging for ABS at different stages of impact property loss against the reciprocal of temperature.

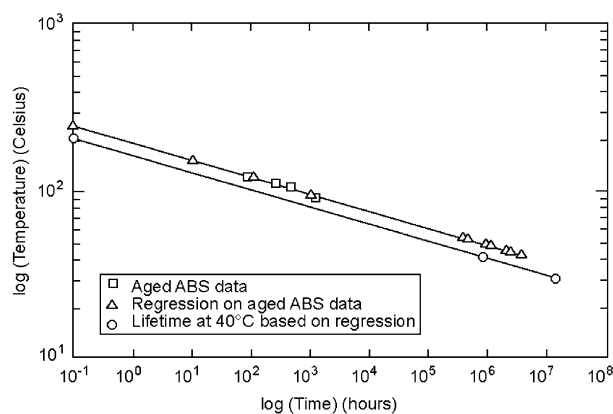


Fig. 17. Loss of impact strength time determined for ABS aged at 40 °C predicted from regression analysis of data at elevated temperatures.

mechanics approach to derive relationships between layer thickness and equivalent surface notch depths.

6. Conclusions

Thermo-oxidative degradation of the PB phase in thick ABS polymer structures after aging at elevated

temperatures is predominantly a surface effect which ultimately precipitates mechanical failure of the polymer. Degradation of the bulk polymer does not occur due to limited oxygen diffusion. For aged ABS under an imposed stress, microcracks initiate from existing flaws in the degraded polymer surface layer. When the degraded layer reaches a depth of 0.08 mm, these cracks are sufficiently large enough to propagate into the bulk of the polymer causing abrupt mechanical failure. Micro-indentation measurements suggest that an increase in Young's modulus in this layer also promotes brittle behaviour.

Degradation of the elastomeric PB phase in ABS is initiated by hydrogen abstraction from the carbon α to unsaturated bonds, producing hydroperoxide radicals, leading to carbonyl and hydroxyl products. Cross-linking of polymer chains is facilitated by the free radicals that are produced. Thermo-oxidative degradation in the PB phase at the surface causes an increase in polymer density, stress hardening and an increase in modulus. Therefore the contribution from the dispersed PB phase to the overall toughening mechanism of ABS, by localised shear yielding and crazing in the SAN matrix, is greatly reduced. Thermal degradation of the SAN phase in ABS also occurs by physical aging and thermo-oxidative degradation, but has only a minor contribution to the deterioration of mechanical properties in ABS.

Thermo-oxidative degradation of ABS is a temperature-dependent process, and mechanical property deterioration is significantly lower at lower aging temperatures. The kinetics of degradation are not typically Arrhenius due to diffusion-limited oxidation effects, and at ambient temperatures both bulk and surface degradation processes exist. A model which accounts for changes in degradation kinetics with temperature is required to predict the ambient mechanical properties of ABS from properties derived after aging at elevated temperatures. Since the most critical degradation process in ABS is thermo-oxidative degradation of the PB phase, performance is dependent on adequate levels and distributions of stabilisers for specific temperature applications.

Acknowledgements

The authors would like to thank Tyco Plastic Pipeline Systems for contributing to the funding of this work.

References

- [1] Wolkowicz MD, Gaggar SK. *Polym Eng Sci* 1981;21(9):571–5.
- [2] Gesner BD. *J Appl Polym Sci* 1965;9:3701–6.
- [3] Shimada J, Kabuki K. *J Appl Polym Sci* 1968;12:665–9.
- [4] Wyzgoski MG. *Polym Eng Sci* 1976;16(4):265–9.

- [5] Salman SR. *Polym Plastics Techn Eng* 1991;30(4):343–9.
- [6] Simha R, Curro JG, Robertson RE. *Polym Eng Sci* 1984; 24(14):1071–8.
- [7] Qi ZN, Wan ZH, Chen YP. *Polym Testing* 1993;12:185–92.
- [8] AS 1146.1, Methods for impact tests on plastics, Part 1: Izod impact resistance. Sydney: Standards Australia, 1990.
- [9] AS 1145, Determination of tensile properties of plastics materials. Sydney: Standards Australia, 1989.
- [10] ISO 188, Rubber, vulcanised-accelerated aging or heat resistance tests, second edition. Geneva: ISO, 1982.
- [11] Faucitano A, Buttafava A, Camino G, Greci L. *TRIP* 1996; 4(3):92.
- [12] Heaps JM. *Rubber and Plastics Age* 1968;October:967–70.
- [13] Clough RL, Billingham NC, Gillen KT. *Polymer durability; Degradation, stabilisation and lifetime prediction: Advances in Chemistry Series 249*. Washington DC: American Chemical Society, 1996.
- [14] Kinloch AJ, Young RJ. Toughened multiphase plastics. Fracture behaviour of polymers. London & New York: Applied Science Publishers, 1983.
- [15] Ramani R, Ramachandra P, Ravichandran TSG, Ramgopal G, Gopal S, Ranganathaiah C. *J Appl Phys A* 1995;60.
- [16] Suzuki T, Kondo K, Hamada E, Chen ZQ, Ho Y. *Radiat Phys Chem* 2001;60:535–40.
- [17] Burn LS, Richards TJ. The Plastics and Rubber Institute Conference, Plastic Pipes IX, 1995.
- [18] Tavakioli SM. ANTEC SPE Conference Preprints 1994:1254.
- [19] Kulich DM, Wolkowicz MD. *Makromol Chem, Macromol Symp* 1993;70/71:407–18.
- [20] Petrie SEB. *J Polym Sci Part A-2* 1972;10:1255–72.
- [21] Petrie SEB. In: *Polymer materials: Relationship between structure and mechanical behaviour*. American Chemical Society for Metals, 1975.
- [22] Stuijk LEC. *Physical aging of amorphous polymers and other materials*. Amsterdam: Elsevier, 1978.
- [23] Tant MR, Wilkes GL. *Polym Eng Sci* 1981;14:874.